Lawrence Berkeley National Laboratory
Recent Work

Title
A STUDY OF OPTICAL MODELS FOR THE ELASTIC SCATTERING OF HEAVY IONS AND RELATED TRANSFER REACTIONS

Permalink
https://escholarship.org/uc/item/03p022zb

Author
Oertzen, W. von

Publication Date
1973-09-01

eScholarship.org Powered by the California Digital Library
University of California

Submitted to
Nucl. Phys.

LBL-1985
Preprint

A STUDY OF OPTICAL MODELS FOR THE ELASTIC SCATTERING OF HEAVY IONS AND RELATED TRANSFER REACTIONS

W. von Oertzen

RECEIVED
LAWRENCE
RADIATION LABORATORY

OCT 16 1973

LIBRARY AND
DOCUMENTS SECTION

September 1973

Prepared for the U. S. Atomic Energy Commission
under Contract W-7405-ENG-48

TWO-WEEK LOAN COPY

This is a Library Circulating Copy which may be borrowed for two weeks. For a personal retention copy, call Tech. Info. Division, Ext. 5545

LAWRENCE BERKELEY LABORATORY
UNIVERSITY OF CALIFORNIA

LBL-1985

DISCLAIMER

This document was prepared as an account of work sponsored by the United States Government. While this document is believed to contain correct information, neither the United States Government nor any agency thereof, nor the Regents of the University of California, nor any of their employees, makes any warranty, express or implied, or assumes any legal responsibility for the accuracy, completeness, or usefulness of any information, apparatus, product, or process disclosed, or represents that its use would not infringe privately owned rights. Reference herein to any specific commercial product, process, or service by its trade name, trademark, manufacturer, or otherwise, does not necessarily constitute or imply its endorsement, recommendation, or favoring by the United States Government or any agency thereof, or the Regents of the University of California. The views and opinions of authors expressed herein do not necessarily state or reflect those of the United States Government or any agency thereof or the Regents of the University of California.

A STUDY OF OPTICAL MODELS FOR THE ELASTIC SCATTERING OF HEAVY IONS AND RELATED TRANSFER REACTIONS*

W. von Oertzen†

Lawrence Berkeley Laboratory
University of California
Berkeley, California 94720

September 1973

ABSTRACT

The elastic scattering ^{16}O ions on ^{54}Fe, ^{64}Ni and ^{208}Pb at energies of ca 20-30 MeV above barrier has been analyzed using the optical model. Different physical assumptions are used to define apriori some of the relevant parameters and the different choices are studied using a first order perturbative treatment of the real potential. DWBA calculations for the different OM potentials are compared for the (^{16}O,^{15}N) and (^{16}O,^{14}C) reaction. It is found that the Q-value dependence and reaction angle dependence of the cross section are influenced in a systematic way by the OM potential parameters.

---

*Work supported under the auspices of the U. S. Atomic Energy Commission.

†On leave from MPJ für Kernphysik, Heidelberg.

1. Introduction

Angular distributions of elastic scattering of heavy ions with two different masses (e.g. ^{16}O on medium mass and heavy nuclei A = 40-208) exhibit a smooth decrease of the differential cross section as a function of angle (for example fig. 1). The deviations from Rutherford scattering (σ_R) can be described in configuration space by essentially two parameters i.e. by an angle (or radius R_0) where the cross section deviates from σ_R and a constant for the exponential slope (see ref. [1]) as function of the minimum distance R,

$$R = \frac{\eta}{k} \left(1 + \frac{1}{\sin \theta/2}\right) \tag{1}$$

$$\frac{\sigma}{\sigma_R} = 1 , \quad R > R_0 ;$$

$$= e^{(R - R_0)/\Delta} , \quad R \leqslant R_0 ; \tag{1a}$$

This fact would actually suggest (as done in ref. [1]) that the scattering could be described by Coulomb scattering with absorption alone.

The amount of information in these angular distributions is very limited. However, details at the break point, where the cross sections often exceeds σ_R by 10-30%, are rather sensitive to the relative magnitude of the attractive nuclear potential and the absorptive potential[2,3].

The differential cross sections have a shape which can be described by Fresnel diffraction formulae[4], corresponding to the absorption of divergent waves. The Coulomb field acts here as a divergent lense and the Coulomb barrier as diffractive edge. Actually, as will be shown later, the real potential, which in conjunction with the Coulomb potential form the diffractive boundary, is very essential for the formation of the Fresnel diffraction pattern (because without the real potential no barrier or edge is produced).

Optical Model calculations are usually rather successful in fitting these angular distributions using a complex potential of Woods-Saxon shape.

$$V(R) = V_0 f(r) + iW f'(r) \quad ;$$

with

$$f(r) = \left(1 + \exp \frac{(r - R_0)}{a_0}\right)^{-1}$$

$$f'(r) = \left(1 + \exp \frac{(r - R_i)}{a_i}\right)^{-1} \qquad (2)$$

and

$$R_{0,i} = r_{0,i} \left(A_1^{1/3} + A_2^{1/3}\right); \quad A_i \text{ nuclear masses.}$$

In many calculations due to the redundancy of the parametrization in the optical model the restrictions $r_0 = r_i$ and $a_0 = a_i$ were used to reduce the number of parameters in the calculation. A typical parameter set which was found to give satisfactory fits to elastic scattering data at energies

between 10-30 MeV above the Coulomb barrier and projectiles like ^{12}C and ^{16}O on nuclei with masses from A_2 = 40-208 is parameter set 2 in Table 1.

However, DWBA calculations for (^{16}O, ^{15}N) and (^{16}O, ^{14}C) reactions at a variety of targets (and Q-values) have shown that the position of the grazing angle is often not correctly described by this standard choice of the optical model, although it gave good fits to the elastic scattering[5,6]. It is well known that transfer reactions are in many cases (in particular in cases of bad matching conditions in angular momentum) more sensitive to details of the optical model[7]. The elastic scattering is usually only sensitive to the very surface of the potential, leading to continuous ambiguities in the parameters of both the real and imaginary potentials[8,9]. The DWBA calculations show a greater sensitivity to these parameters, which is strongest for the (^{16}O, ^{14}C) reaction due to the steep decay of the bound state wave function. The calculations of the (^{16}O, ^{14}C) reaction usually also show the largest descrepancies between calculated and experimental angular distributions (the experimental grazing angle is often 10°-20° smaller compared to the calculated one).

In the present study different choices of the optical model potentials are discussed and their influence of the (^{16}O, ^{14}C) cross section as a representative for transfer reactions are shown. The elastic scattering data analyzed are: 60 MeV, ^{16}O on ^{64}Ni; 60 MeV, 52 MeV, 48 MeV, ^{16}O on ^{54}Fe (refs. [1,10]); ^{18}O on ^{58}Ni at 63.5 MeV (ref. [11]) and ^{16}O on ^{208}Pb at 104 MeV (ref. [12]). DWBA calculations are only shown for the $^{54}Fe(^{16}O, ^{14}C)^{56}Ni$ and $^{44}Ca(^{16}O, ^{14}C)^{46}Ti$ reactions.

2. OM Calculations

2.1. FIRST ORDER TREATMENT OF THE REAL POTENTIAL

For a discussion of the potentials for strongly absorbed particles it can be assumed that the real potential acts as a small perturbation. The scattering potential is thus split into two parts

$$U(R) = \{V_c(R) + iW(R)\} + V_N(R) \quad . \tag{3}$$

The total scattering amplitude can thus be considered to consist of two parts

$$f_N(\theta) = f_{c+W}(\theta) + f_N(\theta) \quad . \tag{4}$$

The first term is calculated in the usual way in the optical model calculation, whereas the amplitude $f_n(\theta)$ is calculated in first order by DWBA

$$f_N(\theta) = \int \chi^{(-)*}_{c+W}(R)\, V_N(R) \int \chi^{(+)}_{c+W}(R)\, dR \quad . \tag{5}$$

The cross sections $|f_{c+W}(\theta)|^2$ and $|f_N(\theta)|^2$ and $|f(\theta)|^2$ (calculated in the usual way) then can be discussed separately (shown in fig. 1). If the Coulomb + imaginary potential describes the elastic scattering data already satisfactorily, a prescription as suggested by the semi-classical model could be used to calculate the elastic scattering (or the absorption) and the contribution of $f_N(\theta)$ should be rather small. In this description the drop-off in the cross section σ/σ_R is assumed to arise due to absorption of

particles (damping of the wave) along the scattering orbit[2])

$$\frac{\sigma}{\sigma_R} \sim \exp\left\{-\frac{i}{\hbar}\int_{\text{orbit}} W(R(t))\ dt\right\};\quad \theta > \theta_0 \ . \qquad (6)$$

This finally leads to the expression (1a) for σ/σ_R .

The imaginary potential of Woods-Saxon shape in this case should have a diffuseness of $a_i \simeq 0.7$ fm, as determined by Christensen et al.[1]) from graphs of σ/σ_R versus R_{min} (using expression (1) and $\Delta = 0.55$). Therefore, in the calculations, potential parameter sets were tried in which a_i was fixed to 0.7 fm.

2.2. THE IMAGINARY POTENTIAL

Calculations were performed with a Coulomb potential and an imaginary potential alone. It was found that a diffuseness of $a_i = 0.7$ fm was indeed necessary to reproduce the fall off of σ/σ_R approximately. These calculations never gave a rise of σ/σ_R at the break point larger than 1.06 or 1.07, whereas most of the data exhibit the typical Fresnel type oscillations with values of σ/σ_R up to 1.30. As already stated in the introduction the oscillatory pattern arises only if an edge (that is the Coulomb barrier) is present. Expression (4) suggests that the oscillatory pattern arises from the interference of the two amplitudes $f_{c+W}(\theta)$ and $f_N(\theta)$.

For a further discussion we assume that $f_N(\theta)$ can be calculated in a semi-classical picture by multiplying the scattering probability with the form factor; defining $V_N(R) > 0$ we have

$$f_N(\theta) = - f_{c+W}(\theta) \quad V_N(R) \tag{7}$$

$V_N(R)$ can be transformed to $V_N(\theta)$ using relation (1). The total amplitude becomes

$$f(\theta) = f_{c+W}(\theta) \ (1 - V(\theta)) \tag{8}$$

and the cross section

$$\frac{d\sigma}{d\Omega} = f^2_{c+W}(\theta) \ (1 - V(\theta))^2 \quad . \tag{9}$$

From expression (9) it becomes clear that: (i) the Fresnel oscillatory structure is very likely an effect which can not be described by a real potential which acts as a first order perturbation only. (ii) The cross section f^2_{c+W} has to be larger than $f^2(\theta)$, the total (or experimental) cross section, if an attraction potential is added to the Coulomb potential (see also fig. 1 and Section d). (iii) The semi-classical prescription (1a) for the calculation of σ/σ_R is probably incorrect because it puts

$$f^2(\theta) \equiv f^2_{c+W}(\theta) \quad .$$

The second possibility for an a priori choice of a parameter is to fix the value of a_i to a rather small value $a_i \simeq 0.2$ fm. Values of a_i in this range have been widely used in the analysis of α-particle elastic scattering on medium weight nuclei[13]). If it is assumed, as has been suggested by Robson and Coworkers[14]), that the imaginary potential reflects

the angular momentum matching conditions between the elastic channel and any other channel which removes flux from the elastic channel, an ℓ-dependent imaginary potential has to be used. As shown by Frahn[15]), the ℓ-dependence of W(R) can be incorporated in the R-dependence, and leads to a smaller diffuseness of the imaginary potential then usually applied. These facts suggest that a small value of a_i should be appropriate.

2.3. THE REAL POTENTIAL

Because of the ambiguities observed in the parametrization with three parameters using the Woods-Saxon shape, the depth of real potential can be chosen nearly arbitrarily, provided the strength of the real potential is the same at the surface. More precisely it was found[16,17]) that the position and the height of the barrier determine primarily the angular distribution. However, using methods based on folding techniques and information from the nucleon-nucleus interaction and the nuclear matter distributions[18]) the depth of real potential can be determined in a consistent way with the depth used for example for α-particle scattering. To achieve this we use the approach of Eisen[18]), who derives the following expression for the depth of the real potential

$$V_0 = \frac{K \cdot A_1 \cdot A_2}{(1 + {}^2a^2/R_0^2)\, r_0^3\, (A_1^{1/3} + A_2^{1/3})} \quad . \tag{10}$$

This expression is essentially the same used for the elastic scattering of light particles. K is here related to the nucleon-nucleon interaction. In the present study it was determined from α-particle potentials and then the

same value was used for the heavy ion potentials describing the scattering of α-particles from mass 40 to 90 [13]. K ranges from 130 to 151. Subsequently, a value of K = 140 was used to derive the depth of the heavy ion potentials using the same parameter r_0 = 1.21 fm. The depth of the real potential determined using these values were for example: $^{16}O + ^{54}Fe$, V_0 = 310 MeV; $^{16}O + ^{208}Pb$, V_0 = 450 MeV. Calculations with these values were done keeping the depth of the real potential fixed (and also the diffuseness of the imaginary potential a_i) and rather satisfactory fits were usually obtained without much adjustment in the parameters r_0 and a_0. The deeper real potentials have the tendency to produce a total potential which is negative ($V_c + V_n < 0$ at small distances) inside the nucleus very similar to the situation with light particles. The total potential is thus more like a well with a barrier in contrast to potentials with values of $V_0 \approx 20$ to 40 MeV.

2.4. RESULTS OF THE OM CALCULATIONS

The different potential sets which gave average fits to the scattering of ^{16}O on ^{54}Fe, ^{64}Ni at 60 MeV and 52 MeV, 48 MeV (the potentials were chosen to fit these 4 data sets) are given in Table 1. Potentials which were adjusted to fit ^{16}O scattering on ^{58}Ni at 63.2 MeV and ^{16}O on ^{204}Pb are given in Table 2.

Figure 1 shows the overall fit achieved to the 60 MeV $^{16}O + ^{54}Fe$ scattering and the cross sections discussed in Section 2.1. - the Coulomb and absorptive part, f^2_{c+W}, and the first order contribution from the real potential f^2_N.

For potentials with a large value of $a_i \approx 0.5 - 0.7$ fm, rather weak imaginary potentials resulted (small W) for a proper fit of the overshoots at

the grazing angle, because only these gave sufficiently weak absorption at the nuclear surface. These potentials also gave in some cases oscillations in the elastic angular distribution at large angles (potential sets 4 and 5) and extremely strong oscillations in DWBA calculations (discussed in the next section) for the $^{54}Fe(^{16}O,^{14}C)^{56}Ni$ reaction similar to those obtained by the Brookhaven group[11]). The corresponding DWBA curves are not shown in fig. 2 because they do not seem to correspond to any observed data.

Potentials with a small value of $a_i \approx 0.2$ fm usually fit the overshoot of σ/σ_R at the grazing angle rather well with simultaneously having sufficiently deep imaginary potentials at small distances. The surface transparency suggested by these choices of parameters seems to be consistent with the observations made by the Brookhaven group[11]).

Although fig. 1 shows that for most potentials the first order treatment of $V_N(R)$ is not justified for larger angles, the plots of fig. 1 do show that $f^2_{c+W}(\theta)$ is usually larger than the experimental cross section and that $f^2_N(\theta)$ has to be the larger, the smaller the slope of $f^2_{c+W}(\theta)$ as function of angle. A small imaginary diffuseness implies a small slope for $f^2_{c+W}(\theta)$ and thus a larger contribution of the real potential. This observation seems to be consistent with the fact that fits of transfer data need a stronger real potential than usually assumed[5,6,10]) (often either the radius parameter r_0 and a_0 where increased - giving a larger value of $V_N(R)$ at the nuclear surface - to achieve a better fit to the data).

3. DWBA Calculations

For a test of the different potentials, calculations of the (^{16}O,^{14}C) reaction on ^{54}Fe at 60 MeV were made because the two proton transfer reactions has a rather steep bound state. This fact makes the (^{16}O,^{14}C) more sensitive to changes of the OM potentials. Also in the (^{16}O,^{14}C) reactions the largest discrepancies with experimental data are observed.

Figure 2 shows the calculations for the different potential sets given in Table 1, and for different Q-values for a fixed bound state. The calculations were performed using the code DWUCK and the Buttle-Goldfarb expansion (no recoil). In the calculations the Hankel function in the form factor and the corresponding normalization constant were replaced by the real bound state in the final channel (E_B = 12.5 MeV, r_0 = 1.4 fm, a = 0.65 fm). The absolute cross sections and the shape of the angular distributions show systematic variations with changes in the potential parameters (these variations are much smaller for (^{16}O,^{15}N) reactions). It can easily be found that the potential set 4a which has a strong contribution from the real potential (fig. 1) has the smallest grazing angle - rather close to the experimental data.

Another important feature is the dependence of the angular distribution on changes in the bound state (i.e. mainly its steepness). Potentials with weak contributions from the real nuclear potential generally give a shift (sometimes no shift) of the grazing angle to larger angles for steeper bound states. This behaviour is expected from a dominance of the Coulomb field, because steeper bound states favour contributions from smaller impact parameters and lead to larger scattering angles (potential sets 1,2). The opposite is

true for potentials like set 4a (in Table 1) which give a shift to smaller angles (5° - 10°) for an increase of the binding energy of the two protons in ^{56}Ni by 6 MeV.

The corresponding effect is observed in a comparison of (^{16}O,^{15}N) and (^{16}O,^{14}C) reactions. In the first reaction a bound state with a smaller steepness leads to a larger grazing angle if potentials like 4a are used, whereas standard potentials give roughly the same grazing angle for the two reactions. As an illustration, fig. 3 shows calculations for the (^{16}O,^{14}C) and (^{16}O,^{15}N) reactions on ^{44}Ca with data[6]) which scan the calcium isotopes ^{40}Ca to ^{48}Ca and thus a span of Q-values of approximately -10.0 to 0 MeV. For the overall features of the angular distributions the charge product and the Q-value have the biggest influence, therefore, calculations for ^{44}Ca are compared with data for all isotopes.

The data are not yet reproduced properly, however, the calculations are closer to the data, than those with potential sets 1 or 2, for example. In this respect it is interesting to note that a change of E_f (or Q-value) by a certain amount would bring the theoretical curves into agreement with experiment ($Q_{theory} \approx Q_{exp}$ + 2 MeV). Thus, a proper choice of the OM potentials does not seem to remove the discrepancy between theoretical and calculated grazing angles observed in (^{16}O,^{14}C) and (^{16}O,^{15}N) reactions.

In the following a possible explanation is proposed. The effective interaction in the DWBA matrix element is in post form $V_{A_1A_2}(r) + V_{A_2c}(r_2) - U^{opt}_{A_1(A_2+c)}(r_f)$; which is the difference between the interactions between the cores A_1, A_2 and core A_2 and transferred particle c, minus the optical potential in the final channel $U^{opt}(r_f)$. We consider

only the Coulomb interaction. Usually the assumption is made that $U^{opt}(r_f)$ cancels completely the interaction $V_{A_1A_2}(r)$. In charged particle transfer this cancellation is usually not achieved for the Coulomb interaction if the "proper" Coulomb interaction in the final channel is used. Because of the importance of the Coulomb field in heavy ion reactions with large values of z, it is very likely that the failure of the usual DWBA calculation is connected with the fact that the Coulomb field in the final channel does not cancel the interaction $V^c_{A_1A_2}(r)$. The difference $\frac{Z_1 \cdot Z_2\, e^2}{r} - \frac{Z_1(Z_2+Z_c)e^2}{r_f}$ (Z_i - charges of the cores) is the larger the more charge is transferred in a reaction. Instead of using a charge product of Z_1Z_2 in the final channel (and obtaining a lower Coulomb barrier) one could rise the final channel energy by the corresponding amount to achieve the necessary energy above the Coulomb barrier. The following relations will give the effective final energy E_f^{eff} to be used in DWBA calculations (E^c stands for Coulomb barrier)

$$E_f - E^c_{A_1A_2} \cong E_f^{eff} - E^c_{A_1(A_2+c)} \quad , \tag{11}$$

$$E_f^{eff} \cong E_f + \frac{Z_c Z_1 e^2}{R_0} \cong E_f + \frac{Z_c}{(Z_2 + Z_c)} \cdot E_f^c \quad . \tag{12}$$

The effective final energy thus has to be larger than the final energy determined by the Q-value. It is larger by the percentage change in the charge of final nucleus times the Coulomb barrier in the final channel (in post representation of matrix element).

Several simple predictions can be made. The difference between standard DWBA calculations and the experiment are the larger, the more charge is transferred in a reaction, the closer the final energy is to the Coulomb barrier (this effect is for example observed in (^{16}O,^{15}N) reactions[19,20]) and (^{12}C,^{11}B) reactions[20]). At high energies above the barrier the discrepancy should disappear (see for example 140 MeV data of ^{208}Pb(^{16}O,^{15}N) ref. [20]). As can be seen from fig. 2 for (^{16}O,^{14}C) reactions, often at more positive Q-values no shift of the grazing angle as function of the Q-value is observed. The same effect is observed experimentally, however, at slightly more negative Q-values. The effective Q-values for the (^{16}O,^{14}C) reaction on the Ca-isotopes for example should be taken 2-3 MeV more positive. The calculations in these cases would agree with the experimental data.

A similar treatment can be given in the prior form of the DWBA matrix element with similar results.

4. Conclusions

The treatment of the nuclear real potential as a first order perturbation of the Coulomb scattering process, gives a simple method to assess the role of the real and imaginary parts of the optical potential. It is suggested that the real potential is usually rather strong at the nuclear surface and can not be treated as a first order perturbation. This fact also implies that the imaginary potential should not describe the main features of the angular distribution as suggested by the semi-classical models[1,2]. In order to achieve a strong contribution of the real potential at the nuclear surface (a necessity to describe a variety of transfer data properly) the cross section $f^2_{c+W}(\theta)$ should be much larger than the experimental cross section. This can be achieved by chosing a small diffuseness of the imaginary potential. Otherwise simultaneously weakly absorbing potentials at small internuclear distances result, which will cause problems in DWBA calculations.

Using these suggestions a certain improvement in DWBA calculations has been obtained. However, the remaining discrepancies between the DWBA curves and experimental data can probably not be removed by choices of OM potentials alone (always assuming that fits to the elastic scattering are obtained simultaneously). It is proposed that these discrepancies are connected to insufficient cancellations of Coulomb terms in the effective interaction of the DWBA matrix element. A simple prescription using an equivalent energy above the Coulomb barrier in the final channel explains qualitatively all discrepancies between DWBA calculations and data. A calculation of the corresponding "indirect contributions" to the transfer cross section as for example discussed in ref. [21]) would be of interest.

Acknowledgments

The author thanks his colleagues at LBL, F. Becchetti, D. Kovar, and H. Homeyer for many discussions. It is also a pleasure to thank B. G. Harvey for the hospitality at the 88-inch cyclotron.

References

1) P. R. Christensen, V. I. Manko, F. D. Becchetti, and R. J. Nickles, Nucl. Phys. A207 (1973) 33; and F. D. Becchetti, P. R. Christensen, V. I. Manko and R. J. Nickles, Nucl. Phys. 203 (1973) 1

2) R. A. Broglia, S. Landowne and A. Winther, Phys. Letters 40B (1972) 293; also R. A. Broglia and A. Winther, Phys. Rev. 4C (1972) 155

3) P. R. Christensen , I. Chernov, E. E. Gross, R. Stockstad and F. Videback, Nucl. Phys. A207 (1973) 433

4) W. E. Frahn, Nucl. Phys. 75 (1966) 577; also Ann. Phys. (N.Y.) 72 (1972) 524

5) H. J. Körner, G. C. Morrison, L. R. Greenwood and R. H. Siemssen, Phys. Rev. C7 (1973) 107; and H. J. Körner, Proceedings of the Symposium on Heavy Ion Transfer Reactions, Argonne, Ill. (1973) Vol. I. p. 9

6) R. H. Siemssen, Proceeding of the Symposium on Two-Nuclear Transfer Reactions, Argonne, ILL. (1972), p. 273

7) N. Austern, "Direct Nuclear Reaction Theories", Wiley Publishing Co., New York (1970)

8) U. C. Voos, W. von Oertzen and R. Bock, Nucl. Phys. A135 (1969) 207

9) E. Krubasik, H. Voit, E. Blatt, H.-D. Helb and G. Ischenko, Z. Physik 219 (1969) 185

10) M. C. Lemaire, Phys. Rev. 7C (1973) 281

11) H. E. Auerbach et al., Phys. Rev. Letters 30 (1973) 1078

12) F. D. Becchetti, D. G. Kovar, B. G. Harvey, J. Mahoney, B. Mayer, and F. Pühlhofer, Phys. Rev. C6 (1972) 2215

13) P. Mailandt, J. S. Lilley, and G. W. Greenless, Phys. Rev. Letters 28 (1972) 1075 and preprint (1973)

14) D. Robson, Symposium on Heavy Ion Scattering, Argonne, Ill. (1971), ANL-7837, p. 239 and references therein

15) W. E. Frahn, Nuovo Cimento 1 (1971) 561

16) M. E. Cage, A. J. Cole, and P. J. Pyle, Nucl. Phys. A201 (1973) 418

17) M. C. Bertin, S. L. Tabor, B. A. Watson, Y. Eisen, and G. Goldring, Nucl. Phys. 167 (1971) 216; also R. VandenBosch, University of Washington, Seattle, Washington, Annual Report (1972)

18) Y. Eisen, Phys. Letters 37B (1971) 33 and references therein.

19) H. J. Körner, G. C. Morrison, L. R. Greenwood, and R. Siemssen, Phys. Rev. C7 (1973) 107

20) D. G. Kovar, B. G. Harvey, F. D. Becchetti, J. Mahoney, D. L. Hendrie, H. Homeyer, W. von Oertzen, and M. A. Nagarajan, Phys. Rev. Letters 30 (1973) 1075

21) W. Tobocman, R. Ryan, A. J. Baltz, and S. H. Kahana, Nucl. Phys. A205 (1973) 193

Table 1

V_0	r_0	a_0	W	r_i	a_i	χ^2	Set N_r
30	1.30	0.45	10	1.25	0.7	$\sim$ 2.0	1
40	1.31	0.45	20	1.31	0.45	$\sim$ 2.0	2
100	1.21	0.57	27	1.35	0.25	$\sim$ 2.0	3*
310	1.11	0.47	13	1.05	0.7	$\sim$ 2.0	4
310	1.20	0.42	32	1.32	0.23	$\sim$ 3.0	4a
30	1.32	0.44	2.5	1.31	0.7	$\sim$ 1.5	5 Similar to 4
310	1.20	0.42	55	1.15	0.20	$\sim$	6* Similar to 4

*Fits identical to 4 and 4a.

Table 2

V_0	r_0	a_0	W	r_i	a_i	χ^2	Data
450	1.21	0.455	43	1.40	0.22	~ 2	^{208}Pb, 104 MeV
450	1.28	0.33	7.0	1.4	0.22	~ 2	^{208}Pb, 104 MeV*
450	1.20	0.42	50	1.15	0.20	~ 1	^{208}Pb, 104 MeV
305	1.21	0.435	7.6	1.40	0.29	~ 2	^{58}Ni, 63 MeV
310	1.20	0.42	28	1.16	0.20	< 1	^{58}Ni, 63 MeV
306	1.21	0.415	7.5	1.32	0.40	< 1	^{58}Ni, 63 MeV
100	1.20	0.51	27	1.33	0.25	~ 1	^{58}Ni, 63 MeV

*Oscillations at large angles.

Figure Captions

Fig. 1. Elastic scattering cross sections for $^{16}O + ^{54}Fe$ at 60 MeV. Top: σ/σ_R. Middle: Coulomb and imagainary potential alone. Bottom: First order contribution of the nuclear potential. The different parameter sets for the optical potentials are given in Table 1.

Fig. 2. DWBA calculations for $^{54}Fe(^{16}O,^{14}C)$ reactions at 60 MeV and different Q-values using the optical model potentials of Table 1 (see also fig. 1).

Fig. 3. Comparison of DWBA calculations for the $^{44}Ca(^{16}O,^{14}C)$ reaction with data, using the optical model potential set 4a (Table 1).

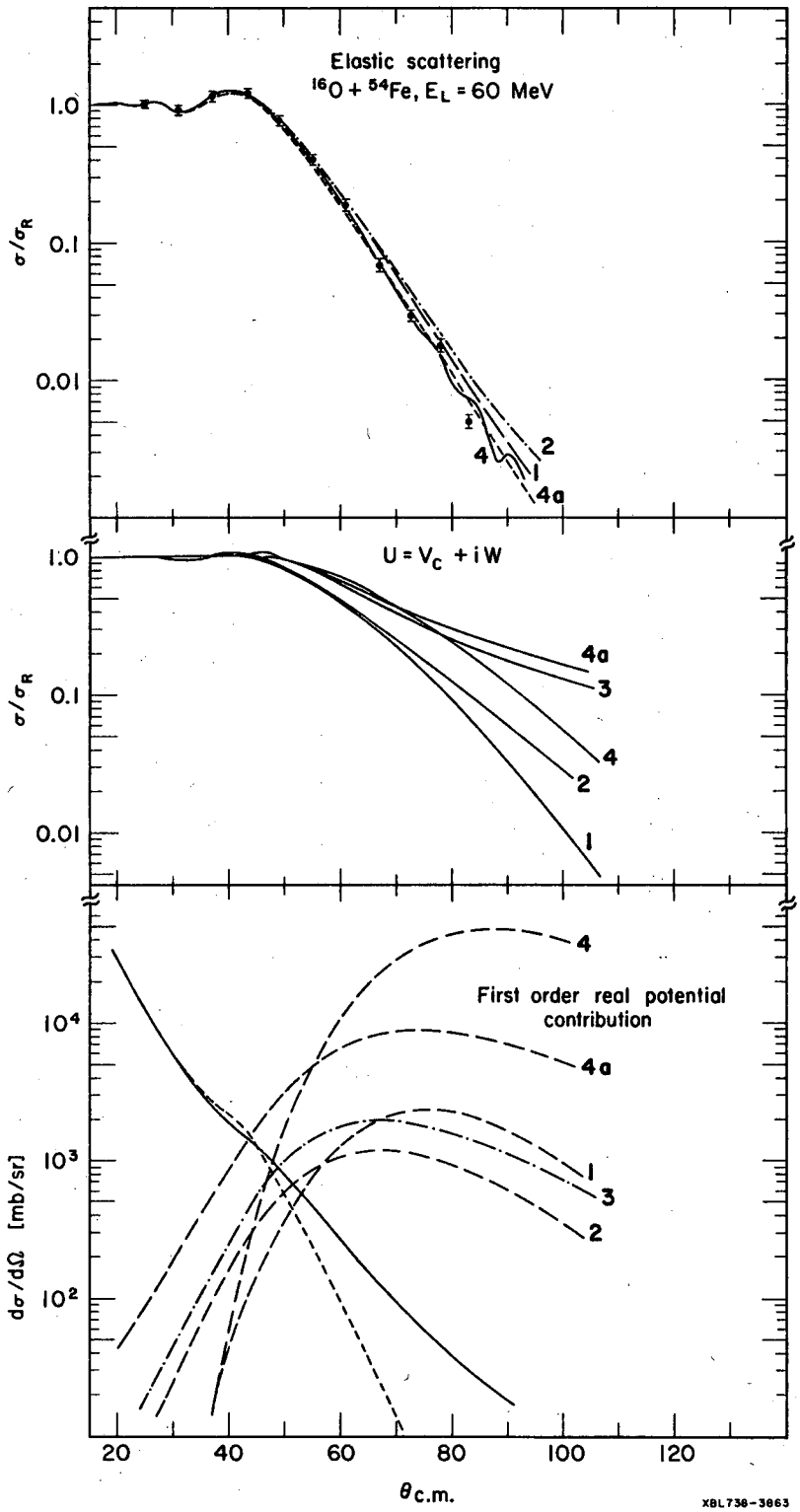
Elastic scattering
$^{16}O + ^{54}Fe$, E_L = 60 MeV
σ/σ_R
1.0
0.1
0.01
4
2
1
4a
$U = V_C + iW$
4a
3
4
2
1
First order real potential contribution
$d\sigma/d\Omega$ [mb/sr]
10^4
10^3
10^2
20
40
60
80
100
120
$\theta_{c.m.}$
XBL736-3663

Fig. 1

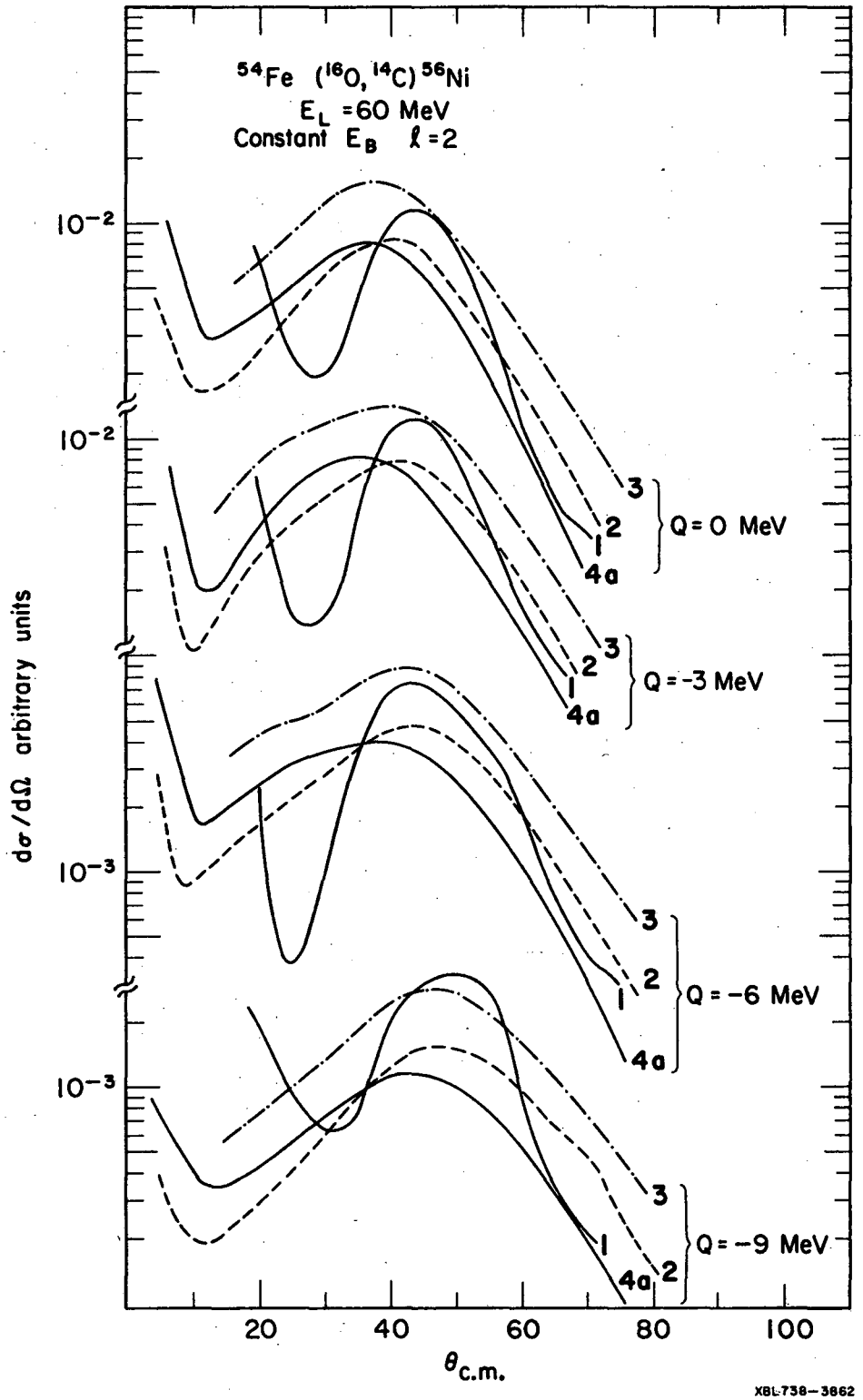
^{54}Fe (^{16}O, ^{14}C) ^{56}Ni
E_L = 60 MeV
Constant E_B ℓ = 2
10^{-2}
10^{-2}
10^{-3}
10^{-3}
$d\sigma/d\Omega$ arbitrary units
3
2
1
4a
Q = 0 MeV
Q = -3 MeV
Q = -6 MeV
Q = -9 MeV
20
40
60
80
100
$\theta_{c.m.}$
XBL738-3862

Fig. 2

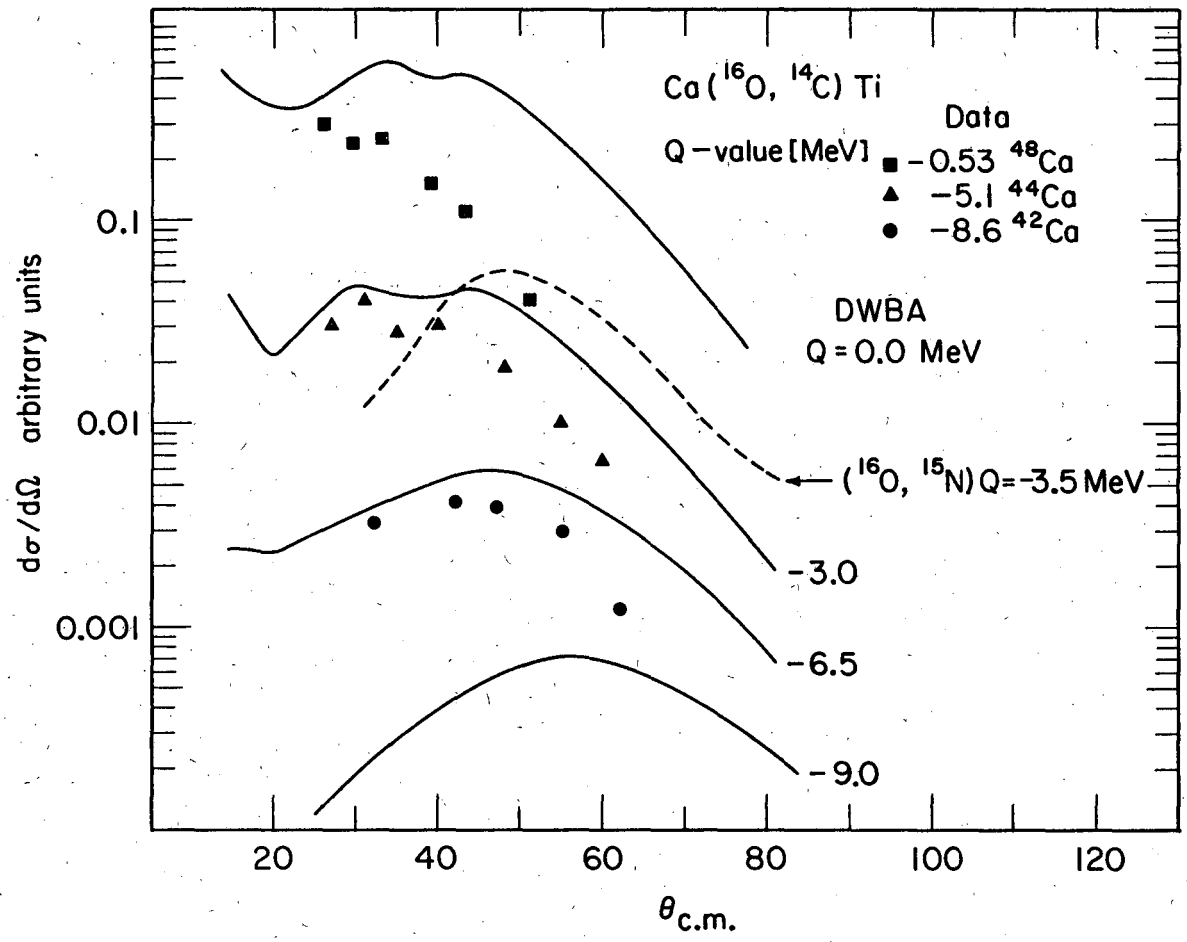
Ca(16O, 14C) Ti
Data
Q-value [MeV]
-0.53 48Ca
-5.1 44Ca
-8.6 42Ca
DWBA
Q = 0.0 MeV
(16O, 15N) Q=-3.5 MeV
-3.0
-6.5
-9.0
dσ/dΩ arbitrary units
0.1
0.01
0.001
20
40
60
80
100
120
θc.m.
XBL 738-3861

Fig. 3

LEGAL NOTICE

This report was prepared as an account of work sponsored by the United States Government. Neither the United States nor the United States Atomic Energy Commission, nor any of their employees, nor any of their contractors, subcontractors, or their employees, makes any warranty, express or implied, or assumes any legal liability or responsibility for the accuracy, completeness or usefulness of any information, apparatus, product or process disclosed, or represents that its use would not infringe privately owned rights.

TECHNICAL INFORMATION DIVISION
LAWRENCE BERKELEY LABORATORY
UNIVERSITY OF CALIFORNIA
BERKELEY, CALIFORNIA 94720